Bonding anisotropy in multiferroic $TbMnO_3$ probed by polarization dependent x-ray absorption spectroscopy

J. M. Chen,[1,a)] J. M. Lee,[1,b)] C. K. Chen,[1] T. L. Chou,[1] K. T. Lu,[1] S. C. Haw,[1] K. S. Liang,[1] C. T. Chen,[1] H. T. Jeng,[2,a)] S. W. Huang,[1,3] T. J. Yang,[3] C. C. Shen,[4] R. S. Liu,[4] J. Y. Lin,[5] and Z. Hu[6]

[1]*National Synchrotron Radiation Research Center (NSRRC), Hsinchu 30076, Taiwan, Republic of China*
[2]*Institute of Physics, Academia Sinica, Taipei 11529, Taiwan, Republic of China*
[3]*Department of Electrophysics, National Chiao Tung University, Hsinchu 30010, Taiwan, Republic of China*
[4]*Department of Chemistry, National Taiwan University, Taipei 10617, Taiwan, Republic of China*
[5]*Institute of Physics, National Chiao Tung University, Hsinchu 30010, Taiwan, Republic of China*
[6]*II. Physikalisches Institut, Universität zu Köln, D-50937 Köln, Germany*

(Received 7 August 2008; accepted 11 December 2008; published online 27 January 2009)

O *K*- and Mn $L_{2,3}$-edges x-ray absorption spectra of orthorhombic $TbMnO_3$ single crystals show strong polarization dependence, in contrast with results of previous experiments on orthorhombic $LaMnO_3$ and $DyMnO_3$ thin films that show nearly isotropic spectral structure. First-principles calculations reveal that $TbMnO_3$ exhibits a zigzag e_g orbital ordering ground state. The highly distorted MnO_6 octahedron and orbital ordering in $TbMnO_3$ produce highly anisotropic Mn–O bonding within the *ab* plane, a frustration of the magnetic ordering, and the formation of complicated incommensurate magnetic structures. © *2009 American Institute of Physics*.
[DOI: 10.1063/1.3064126]

Multiferroic materials in which two or more properties of (anti)ferroelectricity, (anti)ferromagnetism, and (anti)ferroelasticity coexist attract attention because of both their intrinsic scientific interest and prospective applications in novel magnetoelectric and magneto-optical devices.[1] Multiferroicity has been observed in such manganites as $TbMnO_3$, $DyMnO_3$, and $TbMn_2O_5$.[2–5]

$TbMnO_3$, on which we focus here, exhibits an orthorhombically distorted perovskite structure near 300 K and an incommensurate lattice modulation at the Néel temperature (T_N=42 K) corresponding to a sinusoidal antiferromagnetic (AF) ordering along the *b* axis. A second transition into a noncollinear spin arrangement in the spiral phase ($T \sim 28$ K) along the *b* direction is accompanied by ferroelectric ordering with an electric polarization $P \| c$.[2] The appearance of ferroelectricity at the transition into the spiral structure of RMnO$_3$ with R=Tb, Dy, and Gd was microscopically explained in terms of the spin supercurrent according to $\mathbf{P} = \eta \mathbf{e}_{ij} \times (\mathbf{S}_i \times \mathbf{S}_j)$, where P is the electric polarization, $\mathbf{S}_i$ and $\mathbf{S}_j$ are the magnetic moments, $\mathbf{e}_{ij}$ is the unit vector connecting sites i and j, and η is the factor proportional to the transfer integral that is related to the hybridization between Mn 3*d* and O 2*p* states.[6] The magnetoelectric effect is thus closely correlated with noncollinear spin configurations induced by frustrated superexchange interactions that are manipulated with anisotropic electronic structures along the three crystallographic directions and the MnO_6 octahedral distortion of RMnO$_3$.

Although numerous reports of the structural, magnetic, and dielectric properties of RMnO$_3$ (R=Tb and Dy) have appeared,[3,7–10] the electronic structures and anisotropic Mn–O bonding along the three crystallographic directions in $TbMnO_3$ were not examined in detail.[6,11] We investigated the anisotropic bonding of Mn 3*d* states in $TbMnO_3$ single crystals using polarization-dependent x-ray absorption spectroscopy (XAS) at the O *K*- and Mn $L_{2,3}$-edges for three polarizations: $E \| a$, $E \| b$, and $E \| c$. This spectral method is well established to be a powerful tool to probe an electronic structure through its site-selective and symmetry-selective character and has contributed significantly to our present understanding of the local orbital occupation of valence electrons in the ground state.[12–14]

Untwined high-quality orthorhombic $TbMnO_3$ (space group: *Pbnm*, a=5.302 Å, b=5.856 Å, and c=7.401 Å) single crystals were grown by the high-temperature solution method with a PbF_2 flux in a Pt crucible. Two crystal surfaces with crystallographic directions of (100), (010) (i.e., *ab* plane) and (100), (001) (i.e., *ac* plane), respectively, were aligned using an x-ray diffractometer. The O *K*- and Mn $L_{2,3}$-edges XAS spectra were recorded at the Dragon beamline at National Synchrotron Radiation Research Center in Taiwan. Clean crystal surfaces were obtained on cleaving the crystals *in situ* in an ultrahigh vacuum chamber with a base pressure of $\sim 5 \times 10^{-10}$ Torr. The O *K*-edge x-ray absorption spectra were recorded in both the surface-sensitive total-electron-yield (TEY) mode and the bulk-sensitive x-ray-fluorescence-yield (FY) mode. Mn $L_{2,3}$-edge XAS spectra were measured with the TEY mode. Separate $TbMnO_3$ crystals with the same axis showed the great reproducibility of the experimental spectra, indicating the high quality of our crystals.

Figure 1(a) shows the total and site-decomposed densities of states for a hypothetical *A*-type AF structure of $TbMnO_3$ from first-principles electronic structure calculations. The band-structure calculations were performed using the full-potential projected augmented wave method as implemented in the Vienna *ab initio* simulation package (VASP) with a local-density approximation plus an on-site Coulomb interaction U (LDA+U) scheme.[15,16] In these cal-

[a)]Authors to whom correspondence should be addressed. Electronic addresses: jmchen@nsrrc.org.tw and jeng@phys.sinica.edu.tw.
[b)]Also at Department of Electrophysics, National Chiao Tung University, Hsinchu, Taiwan, R.O.C.

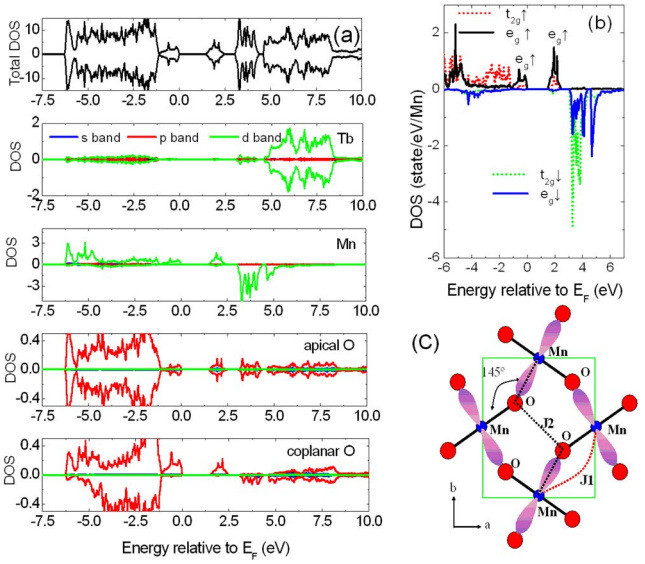

FIG. 1. (Color online) (a) Total and site-decomposed densities of states and (b) partial densities of states of Mn projected onto fivefold 3*d* orbitals for a hypothetical *A*-type antiferromagnetic structure of $TbMnO_3$ calculated with the LDA+*U* method. The parameters in these calculations are described in the text. For each panel the upper half denotes the majority and the lower half the minority spin states. The energy zero is at the Fermi energy (E_f). (c) Schematic drawings of the crystal structure of $TbMnO_3$ with orbital (lobes) ordering within the *ab* plane. J1 represents a ferromagnetic nn superexchange interaction and J2 an antiferromagnetic diagonal nnn superexchange interaction.

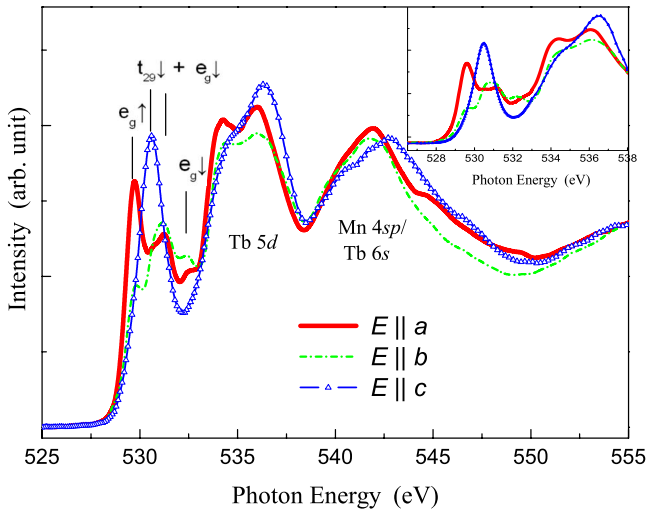

FIG. 2. (Color online) Polarization-dependent O *K*-edge FY XAS spectra of single-crystalline $TbMnO_3$ for polarizations $E\|a$, $E\|b$, and $E\|c$. The assignments of absorption features are described in the text. The inset shows polarized O *K*-edge TEY XAS spectra of $TbMnO_3$.

culations, Coulomb energy $U=5.0$ eV and exchange parameter $J=0.87$ eV for Mn 3*d* electrons were used. As noted from Fig. 1(a), hybridization between the O 2*p* and the Mn 3*d* (or 4*p*) bands is clearly observed. Figure 1(b) displays the partial density of states of Mn projected onto the fivefold 3*d* orbitals. Mn 3*d* bands split into the low-lying t_{2g} (d_{xy}, d_{yz}, and d_{zx}) and high-lying e_g orbitals. Through a strong Jahn–Teller (JT) effect, the $e_g\uparrow$ band splits into two subbands $e_g^1\uparrow$ and $e_g^2\uparrow$ in $TbMnO_3$. The occupied $e_g^1\uparrow$ and unoccupied $e_g^2\uparrow$ (~2 eV above E_f) bands are dominated by $d_{3x^2-r^2}$ and $d_{y^2-z^2}$ orbitals, respectively, in one coplanar Mn ion, whereas they exhibit predominantly $d_{3y^2-r^2}$ and $d_{x^2-z^2}$ characters, respectively, for the other coplanar Mn ion, as represented in Fig. 1(c). The results clearly indicate the formation of an orbitally ordered ground state of $TbMnO_3$ with zigzag aligned e_g orbitals in the *ab* plane, as shown in Fig. 1(c). As for the spin-down channel, one $e_g\downarrow$ band ($d_{3z^2-r^2}$) is mixed with the $t_{2g}\downarrow$ bands at 3–4 eV above E_f, whereas the other $e_g\downarrow$ band ($d_{x^2-y^2}$) is located ~4.5 eV above E_f [Fig. 1(b)].

Figure 2 shows polarization-dependent O *K*-edge XAS spectra of $TbMnO_3$ single crystals recorded at room temperature for three different polarizations: $E\|a$, $E\|b$, and $E\|c$. The inset in Fig. 2 shows polarized O *K*-edge TEY XAS spectra of $TbMnO_3$ crystals freshly cleaved in vacuum. As noted, the spectra in the two different modes are nearly identical. This indicates that the TEY absorption spectrum of crystals freshly cleaved in vacuum also reflects a bulk electronic structure. O *K*-edge XAS spectra were previously observed to have strong polarization dependence for hexagonal $LaMnO_3$ and $DyMnO_3$ thin films but nearly no polarization dependence for orthorhombic $LaMnO_3$ and $DyMnO_3$ thin films.[12] In contrast to previous reports, we observed a strong polarization dependence of O *K*-edge XAS spectra for orthorhombic $TbMnO_3$ crystals, as shown in Fig. 2. To ensure a proper assignment of these features, we took into account the core-hole effect using $Z+1$ approximation in our LDA+*U* calculations.[17] We found no significant difference of the overall shape and relative energy positions of the O 2*p* partial density of states between calculations with core holes ($Z+1$ approximation) and without core holes. Based on the LDA+*U* calculations in Fig. 1, the broad structure located about 535 eV is attributed to O 2*p* states hybridized with Tb 5*d* states, whereas the feature near 542 eV is attributed to a band with mixed Mn 4*sp* and Tb 6*s* character. The pre-edge spectral features below 532.5 eV are due to hybridization of O 2*p* and Mn 3*d* states. The first pre-edge peak at 529.7 eV in Fig. 2 is associated with transitions from the O 1*s* core level into empty O 2*p* states induced by hybridization with unoccupied majority-spin Mn $e_g\uparrow$ bands. We found that the spectral intensity of this peak is significantly stronger for $E\|a$ than $E\|b$, originating from partial occupation of majority-spin Mn $e_g\uparrow$ states. The JT distortion of MnO_6 octahedra in the *ab* plane is accompanied by an orbital ordering, as shown in Fig. 1(c), and produces occupied $d_{3x^2-r^2}/d_{3y^2-r^2}$ and unoccupied $d_{y^2-z^2}/d_{x^2-z^2}$ orbitals projected predominantly along the *b* and *a* directions, respectively. Accordingly, the larger empty O 2*p* projected more along the *a* axis than along the *b* axis. This gives spectral evidence for highly anisotropic Mn–O bonding occurring within the *ab* plane in $TbMnO_3$.[18]

At an energy regime of 530.5–531.5 eV, there is a strong mixture between the minority-spin Mn $t_{2g}\downarrow$ and Mn $e_g\downarrow$ bands hybridized with O 2*p* states, as shown in Fig. 1(b). Unlike majority-spin Mn $e_g\uparrow$ bands, these states are totally unoccupied. One expects the minority-spin Mn $t_{2g}\downarrow$ and Mn $e_g\downarrow$ bands to have an isotropic distribution in the *a* and *b* directions, but the spectral intensity in this energy region shows differences between $E\|a$ and $E\|b$. The predominant spectral intensity at energy ~530.6 eV is out-of-plane polarization ($E\|c$) because the average Mn–O bond length is 2.066 Å in the *ab*-plane and only 1.946 Å for the apical oxygen. This small bond length along the *c*-axis produces strong hybridization between Mn $e_g\downarrow(d_{3z^2-r^2})$–O $2p_z$ and

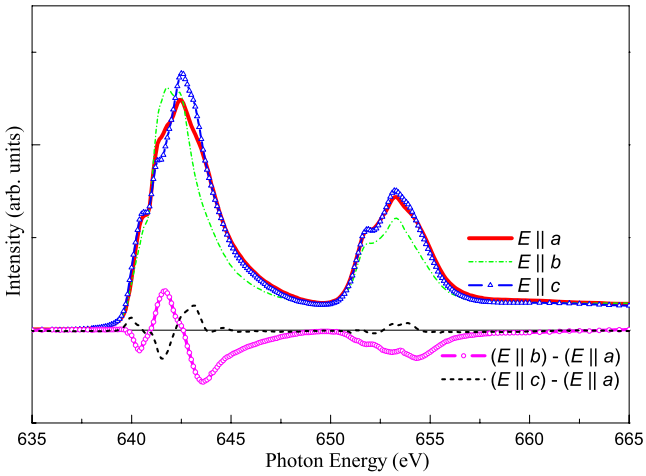

FIG. 3. (Color online) Polarization-dependent Mn $L_{2,3}$-edge TEY absorption spectra of single-crystalline $TbMnO_3$ for three polarizations, $E\|a$, $E\|b$, and $E\|c$, and difference spectra $(E\|b)-(E\|a)$ and $(E\|c)-(E\|a)$.

Mn $t_{2g}\downarrow$–O $2p_z$ responsible for the largest spectral intensity for $E\|c$. The spectral features at ~531.5 and 532.3 eV are found mainly for $E\|a$ and $E\|b$ and are associated with hybridization of O $2p_x$/O $2p_y$ in the *ab* plane with Mn $e_g\downarrow(d_{x^2-y^2})$ bands.

Figure 3 shows polarization-dependent Mn $L_{2,3}$-edge TEY absorption spectra of single-crystalline $TbMnO_3$ for three polarization: $E\|a$, $E\|b$, and $E\|c$. Difference spectra for $(E\|b)-(E\|a)$ and $(E\|c)-(E\|a)$ are also given in Fig. 3. Again in contrast to previous reports,[12] our polarized Mn $L_{2,3}$-edge absorption spectra of orthorhombic $TbMnO_3$ single crystals exhibit a strong polarization dependence along the three crystallographic directions. The polarization-dependent effects between $E\|a$ and $E\|b$ for orthorhombic $TbMnO_3$ are notably larger than between $E\|a$ and $E\|c$. The main peak in polarized Mn $L_{2,3}$-edge XAS spectra of $TbMnO_3$ for the $E\|b$ polarization lies at a lower energy than for polarizations $E\|a$ and $E\|c$. The disparate spectra for polarizations $E\|a$ and $E\|b$ indicate a great anisotropy in Mn 3*d*–O 2*p* hybridization and charge transfer from O 2*p* to Mn 3*d*, reflecting an orbital ordering and a highly anisotropic coplanar Mn–O bonding in $TbMnO_3$ and are consistent with the results for polarization-dependent O *K*-edge absorption spectra in Fig. 2.

For $TbMnO_3$, the MnO_6 octahedron is highly distorted and tilted with an average in-plane Mn–O–Mn bond angle ~145°, to be compared with a much larger value ~155° in $LaMnO_3$ (Ref. 1) as shown in Fig. 1(c). The highly distorted MnO_6 octahedron and orbital ordering in $TbMnO_3$ produces highly anisotropic Mn–O bonding within the *ab* plane, as evident in Figs. 2 and 3, and the frustrated magnetic ordering caused by competition between ferromagnetic nearest-neighbor (nn) superexchange interaction (J1) and antiferromagnetic diagonal next-nearest-neighbor (nnn) superexchange interaction (J2) in the *b*-direction, in particular, spiral spin structures, responsible for the multiferroic behavior in $TbMnO_3$.[19,20]

In conclusion, we demonstrated that polarized O *K*- and Mn $L_{2,3}$-edges x-ray absorption spectra of orthorhombic $TbMnO_3$ single crystals show a strong polarization dependence, reflecting highly anisotropic Mn–O bonding within the *ab* plane in $TbMnO_3$. The highly distorted MnO_6 octahedron and orbital ordering in $TbMnO_3$ produce strongly anisotropic Mn–O bonding within the *ab* plane, a frustrated magnetic ordering, and the formation of complicated incommensurate spiral magnetic structures responsible for the ferroelectricity.

We would like to thank Daniel Khomskii for a critical reading of the manuscript. This research was supported by the NSRRC and the National Science Council of Taiwan under Grant No. NSC 96-2113-M-213-007 and the research in Cologne is supported by the Deutsche Forschungsgemeinschaft through SFB 608.

[1] M. Fiebig, J. Phys. D **38**, R123 (2005).
[2] T. Kimura, T. Goto, H. Shintani, K. Ishizaka, T. Arima, and Y. Tokura, Nature (London) **426**, 55 (2003).
[3] T. Goto, T. Kimura, G. Lawes, A. P. Ramirez, and Y. Tokura, Phys. Rev. Lett. **92**, 257201 (2004).
[4] N. Hur, S. Park, P. A. Sharma, J. S. Ahn, S. Guha, and S-W. Cheong, Nature (London) **429**, 392 (2004).
[5] L. C. Chapon, G. R. Blake, M. J. Gutmann, S. Park, N. Hur, P. G. Radaelli, and S.-W. Cheong, Phys. Rev. Lett. **93**, 177402 (2004).
[6] H. Katsura, N. Nagaosa, and A. V. Balatsky, Phys. Rev. Lett. **95**, 057205 (2005).
[7] T. Kimura, G. Lawes, T. Goto, Y. Tokura, and A. P. Ramirez, Phys. Rev. B **71**, 224425 (2005).
[8] R. Kajimoto, H. Yoshizawa, H. Shintani, T. Kimura, and Y. Tokura, Phys. Rev. B **70**, 012401 (2004).
[9] T. Arima, T. Goto, Y. Yamasaki, S. Miyasaka, K. Ishii, M. Tsubota, T. Inami, Y. Murakami, and Y. Tokura, Phys. Rev. B **72**, 100102 (2005).
[10] N. Aliouane, D. N. Argyriou, J. Strempfer, I. Zegkinoglou, S. Landsgesell, and M. V. Zimmermann, Phys. Rev. B **73**, 020102 (2006).
[11] M. Mostovoy Phys. Rev. Lett. **96**, 067601 (2006).
[12] D.-Y. Cho, J.-Y. Kim, B.-G. Park, K.-J. Rho, J.-H. Park, H.-J. Noh, B. J. Kim, S.-J. Oh, H.-M. Park, J.-S. Ahn, H. Ishibashi, S.-W. Cheong, J. H. Lee, P. Murugavel, T. W. Noh, A. Tanaka, and T. Jo, Phys. Rev. Lett. **98**, 217601 (2007).
[13] M. A. Hossain, Z. Hu, M. W. Haverkort, T. Burnus, C. F. Chang, S. Klein, J. D. Denlinger, H.-J. Lin, C.-T. Chen, R. Mathieu, Y. Kaneko, Y. Tokura, S. Satow, Y. Yoshida, H. Takagi, A. Tanaka, I. S. Elfimov, G. A. Sawatzky, L. H. Tjeng, and A. Damascelli, Phys. Rev. Lett. **101**, 016404 (2008).
[14] M. Mertz, G. Roth, P. Reutler, B. Büchner, D. Arena, J. Dvorak, Y. U. Idzerda, S. Tokumitsu, and S. Schuppler, Phys. Rev. B **74**, 184414 (2006).
[15] G. Kress and D. Joubert, Phys. Rev. B **59**, 1758 (1999).
[16] A. I. Liechtenstein, V. I. Asimov, and J. Zaanen, Phys. Rev. B **52**, R5467 (1995).
[17] M. Nyberg, Y. Luo, L. Triguero, L. G. M. Pettersson, and H. Ågren, Phys. Rev. B **60**, 7956 (1999).
[18] J.-Y. Kim, T. Y. Koo, and J.-H. Park, Phys. Rev. Lett. **96**, 047205 (2006).
[19] T. Kimura, S. Ishihara, H. Shintani, T. Arima, K. T. Takahashi, K. Ishizaka, and Y. Tokura, Phys. Rev. B **68**, 060403 (2003).
[20] D. Senff, P. Link, K. Hradil, A. Hiess, L. P. Regnault, Y. Sidis, N. Aliouane, D. N. Argyriou, and M. Braden, Phys. Rev. Lett. **98**, 137206 (2007).